HHS Public Access

Author manuscript

Metabolomics. Author manuscript; available in PMC 2023 October 30.

Published in final edited form as:

Metabolomics. ; 16(10): 106. doi:10.1007/s11306-020-01729-4.

Changes in lipid profiles of epileptic mouse model

Alicia Johnson[1], **Ryan A. Grove**[1], **Deepak Madhavan**[2], **Cory H. T. Boone**[1], **Camila Braga**[1], **Hannah Kyllo**[2], **Kaeli Samson**[3], **Kristina Simeone**[3], **Timothy Simeone**[3], **Tomas Helikar**[1], **Corrine K. Hanson**[4], **Jiri Adamec**[1]

[1]Department of Biochemistry, University of Nebraska-Lincoln, Lincoln, NE 68588, USA

[2]Department of Neurological Sciences, University of Nebraska Medical Center, Omaha, NE 68198, USA

[3]Department of Pharmacology, Creighton University School of Medicine, Omaha, NE 68178, USA

[4]College of Allied Health Professions, University of Nebraska Medical Center, Omaha, NE 68198, USA

Abstract

Introduction—Approximately 1% of the world's population is impacted by epilepsy, a chronic neurological disorder characterized by seizures. One-third of epileptic patients are resistant to AEDs, or have medically refractory epilepsy (MRE). One non-invasive treatment that exists for MRE includes the ketogenic diet, a high-fat, low-carbohydrate diet. Despite the KD's success in seizure attenuation, it has a few risks and its mechanisms remain poorly understood. The KD has been shown to improve metabolism and mitochondrial function in epileptic phenotypes. Potassium channels have implications in epileptic conditions as they have dual roles as metabolic sensors and control neuronal excitation.

Objectives—The goal of this study was to explore changes in the lipidome in hippocampal and cortical tissue from Kv1.1-KO model of epilepsy.

Methods—FT-ICR/MS analysis was utilized to examine nonpolar metabolome of cortical and hippocampal tissue isolated from a Kv1.1 channel knockout mouse model of epilepsy (n = 5) and wild-type mice (n = 5).

Results—Distinct metabolic profiles were observed, significant ($p < 0.05$) features in hippocampus often being upregulated ($FC \geq 2$) and the cortex being downregulated ($FC \leq 0.5$). Pathway enrichment analysis shows lipid biosynthesis was affected. Partition ratio analysis revealed that the ratio of most metabolites tended to be increased in Kv1.1−/−. Metabolites in hippocampal tissue were commonly upregulated, suggesting seizure initiation in the hippocampus.

✉ Jiri Adamec, jadamec2@unl.edu.

Author contributions A.J., R.A.G., D.M., C.H.T.B., H.K. and K.Sa. carried out experiments; A.J., R.A.G., D.M., C.H.T.B., C.B., K.Si., T.S., T.H., C.K.H. and J.A. performed data analysis and interpretation; A.J. and J.A. wrote paper with input from all the authors.

Compliance with ethical standards

Conflict of interest The authors declare no competing financial interests.

Electronic supplementary material The online version of this article (https://doi.org/10.1007/s11306-020-01729-4) contains supplementary material, which is available to authorized users.

Aberrant mitochondrial function is implicated by the upregulation of cardiolipin, a common component in the mitochondrial membrane.

Conclusion—Generally, our study finds that the lipidome is changed in the hippocampus and cortex in response to Kv1.1-KO indicating changes in membrane structural integrity and synaptic transmission.

Keywords

Seizure; Drug resistant epilepsy; Metabolomics; Lipids; Metabolic profiling

1 Introduction

Epilepsy is a progressive, chronic neurological disorder characterized by hypersynchronous electrical activity resulting in seizures. Approximately 70 million people worldwide have been diagnosed with epilepsy with 30% of all patients having medically refractory epilepsy (MRE), or are resistant to traditional AEDs (Kalilani et al. 2018). The few treatments available for MRE include surgical removal of epileptic tissue which carries risk of interfering with normal brain function (Kelly and Chung 2011). Another is a vagal nerve stimulator (similar to a pacemaker), but carries the risk of interfering with speech or infection. A non-invasive treatment is the ketogenic diet (KD) (Huttenlocher 1976). The KD is a high-fat, low-carbohydrate diet that has shown success in long term seizure attenuation, particularly in adolescents (Huttenlocher 1976). However, the treatment is associated with risks such as palatability with patients, renal damage, and ketoacidosis. Unfortunately, the molecular mechanisms of KD and its impact on MRE remain poorly understood. Although recent findings suggest that ion channels and neurotransmitter functions may be related to metabolic dysfunction in MRE, it is also suggested that the KD acts by providing an alternative metabolic energy source through increased production of ketone bodies (i.e. β-hydroxybutyrate and acetoacetate) (Lutas and Yellen 2013). With the effectiveness of the KD affecting changes in metabolism, MRE may be a result of metabolic disfunction rather than neurotransmitter function. This is also supported by the fact that alterations in redox balance and mitochondrial dysfunction have been considered as hallmarks of epilepsy (Pearson-Smith and Patel 2017).

Potassium channels have emerged as a drug target with AEDs (Stas et al. 2016). These drugs often control neuronal excitability by increasing the open probability of potassium channels to maintain membrane resting potential. Potassium channels act to limit the length of action potentials and maintain the membrane potential. Voltage-gated potassium (Kv) channels could serve as a potential target due to their dual role as metabolic sensors and regulation of neuronal excitation (Nichols 2006). The Kv1.1 channel, encoded by the *KCNA1* gene, is located at the axon in the hippocampus where it is involved in propagation of action potentials and neurotransmitter release (Simeone et al. 2014a, b). When Kv1.1 is ablated in mice, it can cause epileptic symptoms resembling temporal lobe epilepsy (Robbins and Tempel 2012; Wenzel et al. 2007). The Kv1.1 knockout (KO) model resembles several other types of epileptic conditions, making it a clinically relevant model to study metabolic abnormalities in epilepsy (Simeone et al. 2014a, b). This model has also been used to study effects of the KD on metabolism in epilepsy and any additional impacts on

seizure frequency (Kim et al. 2015). Further, supplementation with metabolic intermediates improved mitochondrial function in mitochondria isolated from Kv1.1- KO mice (Simeone et al. 2014a, b). These studies indicate that changes in metabolism play an important role in seizures. While majority of studies have focused on the targeted polar metabolome (for review, refer to Mcdonald et al. 2018), the effects of the nonpolar lipid metabolome in epilepsy is relatively understudied.

Lipids represent approximately 10% of the brain's total mass (Naudí et al. 2015). Considering this nontrivial portion of mass, they have many functions including regulation in membrane structure, neurotransmitter release, energy metabolism, and as messengers in signaling cascades. With lipids playing a potentially important role in almost every aspect of neuronal function, it is pertinent to develop a deeper understanding of the function of lipids as it relates to neurological diseases. Evidence of dysregulated lipid metabolism has been observed in age-related neurological diseases (Dodge et al. 2013; Wenk 2005). Changes in membrane structure have been shown in several epileptic models as well (Turker et al. 2014; Kunduri et al. 2018). It has been observed that there are regional differences in lipid composition in the brain, even within the same structure (i.e. ventral hippocampus vs. dorsal hippocampus) (Miranda et al. 2019). Further, regional differences in lipid peroxidation have been observed in rat brain in response to aging (Baek et al. 1999). With regional differences in lipid composition and metabolism, some may be more impacted by seizure activity than others. An aspect of epilepsy that remains unexplored is the impact of structural and functional connections in the brain on seizure initiation and severity. The interconnectivity of hippocampal and cortical regions are critical to seizure initiation and propagation (Vismer et al. 2015). While the hippocampal gyrus is often regarded as a "seizure gate", there are certain regions within the brain that support the hypersynchronous activity of seizures and data has shown that when these regions (or connections) are disrupted, seizure activity is decreased (Vismer et al. 2015; de Guzman et al. 2004). Therefore, by studying the role of lipids in epileptic conditions, potential future therapeutic targets and/or mechanisms of seizure generation can be identified. In this study, FT-ICR/MS analysis have been employed to observe changes that occur in the lipidome of hippocampal and cortical tissue isolated from a Kv1.1 KO model of epilepsy. Both regions exhibited distinct lipidomic profiles. Further statistical and pathway analysis have identified glycerophospholipids as a major lipid class. This indicates rearrangement of the membrane composition altering its fluidity and permeability—alterations reported in various neurodegenerative disorders(Turker et al. 2014; Sooderberg et al. 1992).

2 Materials and methods

2.1 Animal studies/mouse tissue collection

All protocols were performed in accordance with the United States Public Health Service's Policy on Humane Care and Use of Laboratory Animals and approved by Creighton University's Institutional Animal Care and Use Committee. Hippocampus and cortex tissue sections were harvested from C3HeB/FeJ wild-type (n = 5) and Kv1.1 KO female mice (n = 5) aged between 44 and 50 days as described previously(Roundtree et al. 2016). For KO mice, seizure frequency and severity have been previously established for this model with

approximately 7 seizures per day, sharp pathological wave (SPW) duration of approximately 80 ms and high frequency oscillations in the range of 200–600 Hz (Simeone et al. 2014a, b; Roundtree et al. 2016; Fenoglio-Simeone et al. 2009). Mice were euthanized using a MMW-05 Muromachi Microwave Fixation system (Muromachi Kikai Co.) to minimize metabolic changes through heat inactivation of enzymatic activity (Jernerén et al. 2015). Tissue samples were stored at − 80 °C until metabolite extraction.

2.2 Extraction of non–polar metabolites

Non-polar metabolite extraction was done using a modified Folch method (Folch et al. 1957). Briefly, ZrO bashing beads and 150 mM NaCl in 75% MeOH were added to hippocampal or cortical tissue in an Eppendorf tube at a 1:2:0.5 ratio of the following: tissue (mg)/150 mM NaCl in 75% MeOH (μL)/ZrO beads (μg). The brain tissue was homogenized for 2 min at high speed (power setting of 10) in a Bullet Blender (Next Advance, NY) and homogenate (20 μL) moved to the new tube with 180 μL of 150 mM NaCl and 1 mL of chloroform/MeOH (2:1, v/v) containing 0.01% butylated hydroxytoluene. Sample was then vortexed for 2 min and allowed to stand for 30 min at room temperature. To further separate phases, the sample was centrifuged at 7800×*g* for 5 min and the lower phase transferred into the new tube. Extracted lipids were dried under N_2 stream and dissolved in 20 μL of methanol for LC–MS analysis.

2.3 LC–FT–ICR–MS analysis of lipids

Metabolites were analyzed using an Agilent 1100 series HPLC connected to a Bruker 7.05 T FT-ICR mass spectrometer. Separation of metabolites was performed on an ACE5 C8 (100 × 2.1 mm) column at 100 μL/min flow rate over 60-min chromatographic run. Mobile phase A consisted of 0.1% formic acid (FA) and 10 mM ammonium acetate in water while mobile phase B consisted of 0.1% FA and 10 mM ammonium acetate in isopropanol/acetonitrile (50/50; v/v). With a sample injection of 5 μL, the following chromatographic conditions were used: initial conditions 30% B for 1 min, then increased to 100% B over 24 min and held for 20 min. To re-equilibrate column, the system returned to the initial conditions (30% B) in 2 min and continue with washing for 13 min. MS was operated in positive mode with acquisition range 118–1800 m/z and 0.2 s ion accumulation time. Estimated resolving power was 78,000 at m/z 400. Following MS conditions were used: a capillary voltage of 4500 V and an end plate offset of −500 V; the dry temperature was set at 180 °C; the dry gas flow was maintained 4 L/min.

2.4 Data processing

LC–MS data was converted into mzXML format using CompassXport v. 3.0.6. (Bruker Daltonics) software. Peak detection, alignment, normalization, and retention time collection analyses were done using mzMine (Pluskal et al. 2010) and the following parameters: Minimum Standard Intensity: 500,000; Retention time (RT) tolerance: 0.2 min; Peak duration range: 0.2–2 min; Derivatization threshold: 99%; FTMS Shoulder peak filter: 10,000; m/z tolerance: 10 ppm. Retention times, peak areas, and m/z values were exported to Excel tables for further processing. Upon further evaluation of the individual peak chromatograms of the samples and blanks, only the peaks with an RT between 9 and 37 min were used for further analysis. As expected for lipids and gradient used in the

method, no significant peaks with reproducible retention times were detected until 9 min of gradient. Peaks detected after 37 min were, on the other hand, strongly influenced by noise signal present (found in both samples and blanks) and potentially compromising quantitative analysis through affecting ionization efficiency. To determine presence or absence of the features to specific groups, feature must be present in 60% of the samples within the group to be considered as the "true" feature. The partition of the detected features was visualized using Venny 2.1 and Venn Diagram (Oliveros 2007).

2.5 Statistical analysis

Details on statistical analysis have been provided in "Supplementary Methods". Briefly, Multivariate and univariate analyses were done using Microsoft Excel and Metaboanalyst 4.0 (Chong et al. 2019). One-way ANOVA was used to determine if features varied by tissue type. Similarly, one way ANOVA was also used to determine if features varied by genotype. Statistics for this analysis have been provided in Supplemental Table 4. Following data normalization and scaling, PLS-DA plots, heatmap, hierarchical clustering and volcano plots were generated using Metaboanalyst for all analyses. For tissue partition analysis, the "in sample" ratio between hippocampus and cortex from the same mouse was calculated (KO_{Hippo}/KO_{Cortex} and WT_{Hippo}/WT_{Cortex}) and used in statistical analysis. Student's *t* test ($p < 0.05$) and a fold change of ≥ 2 and ≤ 0.5 were used to determine differentially expressed metabolites which were then tentatively identified using Human Metabolome Database (HMDB 2018 version) and Lipid Maps structure database with mass tolerance of 10 ppm or ± 0.01 m/z in both databases, respectively (Wishart et al. 2017; Sud et al. 2007). Positive mode ion adducts, $[M + H]^+$ and $[M + NH_4]^+$ were selected for identification. The identifier with the lowest mass difference was chosen as the representative ID for this paper.

2.6 Pathway analysis

Corresponding KEGG IDs of the tentatively identified features were used in the Metaboanalyst Pathway Analysis module and the Reactome pathway database. In Metaboanalyst, hypergeometric test and relativebetweenness centrality were the algorithms used in overrepresentation analysis and pathway topology analysis, respectively. Statistics for Reactome pathway analysis have been provided in Supplemental Table 3.

3 Results

3.1 Overall analysis and data overview

Using a genetic Kv1.1-KO mouse model of epilepsy, nonpolar metabolites were extracted from hippocampal (WT, n = 5; KO, n = 5) and cortex (WT, n = 5; KO, n = 5) tissue female mice. These regions were chosen due to initiation of generalized seizures in the hippocampus and subsequent spreading to the cortex. Overall, 4323 features were detected when comparing both tissue types and genotypes. These features show 98.7% (4266 features) overlap between all groups with 31 metabolites being unique to Kv1.1−/− cortical tissue and wild-type hippocampal and cortical tissue (Fig. 1a). Six metabolites were unique to cortical tissue of both genotypes and two metabolites were unique to wild-type cortex. Finally, 17 metabolites were unique to cortical tissue of both genotypes and Kv1.1−/− hippocampal tissue. Hierarchical clustering suggested a trend of clustering based on

genotype, however, this has some variability (Fig. 1b). PLS-DA analysis showed variability which may be attributed to a high number of features (Fig. 1c). As a result, tissues were analyzed separately in Metaboanalyst.

3.2 Lipid partition between hippocampus and cortex

Because hippocampal and cortical tissues have highly connected circuitry and are thus, communicative, the partition (or balance) of the individual lipid species in these tissues may play an important role in the seizure onset. Therefore, the “in sample” ratios (referred to as partition ratios hereon) of the lipids between hippocampus and cortex were calculated and statistically analyzed (Table 1). The partition analysis revealed, from the 4352 features that were detected, that the ratio 29 metabolites were significantly changed ($p < 0.05$) and had a fold change of ≥ 2 and ≤ 0.5 (Table 1). Twenty-two ratios had increased in response to the deletion of Kv1.1, indicating a higher intensity in the hippocampus; seven had decreased, indicating a higher intensity in the cortex. The classes of the metabolites consisted of glycerophospholipids and glycerolipids. The upregulation of different lipid species could be indicative of increased flux through lipid production and signaling pathways or of structural remodeling of the cell membrane. Based on the m/z and RT of the specific lipid classes, 16 features were tentatively identified. For unidentified features, it can be suggested that they can also be attributed to glycerophospholipids (mostly cardiolipin) due to their m/z values and RT.

3.3 Analysis of non–polar metabolome of Kv1.1 null mice reveals changes in phospholipid levels in hippocampal tissue

In order to examine if there are differentially expressed metabolites that may affect seizure susceptibility in the Kv1.1 KO genotype, additional statistics were done on the tissues separately. Of the features detected in the hippocampus, Students t-test and fold change analyses revealed that 66 significantly changed features (p value < 0.05) with a fold change of $0.5 <$ or > 2 and (Fig. 2a). PLS-DA appeared to separate WT and KO samples into two distinct groups (Fig. 2b). When these features are visualized on a heatmap, they can be hierarchically clustered into WT and KO groups (Fig. 2c) suggesting lower “in group” variation and metabolic alterations contributed primarily to the genotypes and pro-epileptic conditions. For tentative identification, both the m/z and RT of the specific lipid classes, were used. Of the compounds, 22 of them were tentatively identified using HMDB and LMSD database searches. Results showed that many of these compounds consisted of the as glycerophospholipid including phosphatidylethanolamine (PE), phosphatidylcholine (PC), and cardiolipins (CL) apart from a glycerolipid (Supplementary Table 1). Of the identified compounds, all were upregulated except for a phosphoglycerol. In addition, it can be suggested that the unidentified features can also be attributed to these lipid classes due to their m/z values and RT. Following fold change analysis, 58 features were upregulated and consisted of glycerophospholipids (mainly cardiolipin and phosphatidylethanolamines) while the 8 downregulated features consisted of phosphatidylglycerols or remain unidentified.

3.4 Analysis of non–polar metabolome reveals changes in phospholipid composition in cortex tissue

Like hippocampus analysis, these samples can be grouped into WT and KO in all pairwise comparison, PLS-DA analysis and hierarchical clustering (Fig. 3a–c). Seventy-two features had at least a fold change ≥ 2 and a p value < 0.05 with 11 being upregulated and 61 being downregulated. Of those, 26 metabolites were tentatively identified using both LipidMaps and HMDB (Supplementary Table 2). However, due to the m/z values and RT, the unidentified features are likely to be glycerophospholipids. All phosphatidylinositols, phosphatidylserines, and some phosphatidylethanolamines were downregulated while a few cardiolipins and phosphtidylcholines were upregulated. This could be attributed to the hippocampus being the site of seizure initiation thus causing a breakdown between the communication between hippocampal and cortical tissue.

3.5 Pathway enrichment analysis and overall patterns in fold changes

Using Metaboanalyst and Reactome pathway enrichment analyses yielded similar results with Reactome providing detail on specific pathways affected. Generally, glycerophospholipid and sphingolipid synthesis were impacted across both tissue types (Fig. 4a). Specifically, phosphatidylserine synthesis, phosphatidylglycerol synthesis and acyl chain remodeling of cardiolipin and phosphatidylethanolamine were changed (Fig. 4b). Further, comparing all significant species' differential regulation found in all groups to other groups in which the lipid was not significant yielded interesting observations (Fig. 5). First, the hippocampus generally seemed to follow the overall pattern of the partition ratio, with most metabolites and partition ratios being upregulated in Kv1.1-KO mice. This indicates that the increase observed in most partition ratios upon Kv1.1-KO arise due to changes within the hippocampus. Additionally, the cortex continued its trend with most metabolites, including non-significant ones, being downregulated.

4 Discussion

Epilepsy is a chronic neurological disorder that is characterized by abnormal neuronal excitation. Although epileptic phenotypes have been shown to be mediated by the KD, which ultimately results in a metabolic fuel switch (Lutas and Yellen 2013), the molecular mechanism of this effect is unknown. The Kv1.1-KO mouse model of epilepsy, which lacks some potassium channels critical to metabolic sensing and neuronal function through maintenance of negative membrane potential (Nichols 2006), has been demonstrated to respond to the KD. Therefore, the analysis of nonpolar metabolites in brain tissue may provide insights into metabolic dynamics and indicates a potential effect of the KD on the epileptic phenotype.

To evaluate overall profiles of lipids in two epilepsy relevant tissues, hippocampus and cortex, and genotypes (WT and Kv1.1 KO), multivariant analysis was performed. Vast majority of the detected features (98.7%; 4226 features) were found in all samples (Fig. 1). Statistical analysis revealed genotype over tissue clustering with a minimum of significantly changed features identified. This suggests that detailed, tissue specific analyses were necessary. Additionally, simultaneous analysis of cortex and hippocampus

tissues from the same animal, allows for a unique “in sample” partition analysis of the individual lipids in those tissues. It has been demonstrated that hippocampal and cortical brain neural connections can allow for the propagation and initiation of seizures (Barbarosie and Avoli 1997; Bragin et al. 1999). Additionally, the ratio of lipid classes rather than overall composition can give cellular membranes different functions and characteristics (Farooqui et al. 2000). To determine if an imbalance of lipids between the cortex and the hippocampus regions could contribute to seizure propagation, the individual ratios of all features from the same animal have been calculated and statistically analyzed. The ratios of 29 metabolites (Table 1) were significantly ($p < 0.05$) changed with a fold change of > 2 and < 0.5. Some metabolites were tentatively identified as glycerophospholipids and glycerolipids. Many of the metabolites were found to be upregulated upon Kv1.1-KO, indicating a potential need for membrane remodeling and/or increased flux through lipid production pathway to be used in downstream signaling pathways. Probably the most interesting tentatively identified lipids were DG(36:3) and a few cardiolipins.

Reduced levels of DG(36:3) was discovered to be a marker of sleep restriction (Weljie et al. 2015). Interestingly, the Hippocampus/Cortex ratio of this metabolite was found to be almost two-fold decreased in Kv1.1 KO mice (Table 1). Although these results are consistent with original findings, it may suggest that the changes in DG(36:3) are tissue specific rather than overall concentration. Insufficient sleep has been reported to be a comorbid condition with epilepsy, often increasing severity and frequency of seizures (Roundtree et al. 2016). The Kv1.1 KO model used in this study has also been reported to exhibit longer periods of activity during times of rest, indicating troubles with sleeping (Roundtree et al. 2016). The impact that DG(36:3) may ultimately have on epilepsy remains uncertain. However, other studies have suggested that diacylglycerol kinases (DGKs) may impact neurotransmitter release and have been implicated in seizures and other neurological disorders (Shirai and Saito 2014).

The partition ratio of cardiolipin(CL), was upregulated in response to Kv1.1 knockout (Table 1). CL is involved in mitochondrial function and complex formation and has also been identified as a target for redox function in brain injuries (Ji et al. 2012; Zhang et al. 2005). These molecules are a critical component of the inner mitochondrial membrane (IMM) that aids in mitochondrial bioenergetics through stabilization and organization of IMM proteins (Paradies et al. 2014). Oxidized CL has been shown to induce mitochondrial permeability transition pore opening which is also induced by calcium influx. Finally, ATP dynamics are often disrupted in epilepsy (Lutas and Yellen 2013; McDonald et al. 2018). Within the Kv1.1-KO model of epilepsy, ketone bodies (products of the ketogenic diet) has been demonstrated to raise mitochondrial permeability thresholds within the hippocampus (Kim et al. 2015). The upregulation of CL ratios could be attributed to several factors including tissue specific irreversible modifications of CLs or direct, tissue specific increase in CL production. In general, the epileptic seizures are accompanied by high levels of oxidative stress, usually originating in mitochondria and its environment. This can lead to the oxidation of CLs proximal to these sites. In this case, the cortex tissue would be primarily affected by oxidation decreasing the CL levels and increasing the Hippocampus/Cortex ratios. Increased CL oxidation and subsequent accumulation in cortex tissue may also contribute to seizure initiation. Alternatively, the metabolic stress that occurs in seizures may

lead to the tissue specific increased production of CL in order to stabilize the mitochondrial membrane proteins, maintain ATP production, and to prevent permeability pore opening. The third and most probable scenario includes both mechanisms.

Although the balances of lipid partition are important, their relative concentrations and patterns can be highly complementary and indicative of potential metabolic changes. In the tissue specific analysis, most of the tentatively identified, significantly changed compounds consisted of glycerophospholipids, many of them being (PI, PE, CL) (Supplementary Table 1 and 2). Together with the tentatively identified molecules in the partition analysis, the most affected pathway were related to lipid biosynthesis and remodeling (Fig. 4a and b) When observing the fold change in response to the knockout, metabolites tended to be upregulated in the hippocampus and downregulated in the cortex with some exceptions (Supplementary Table 1 and 2). These results, together with partition analysis, where many metabolites were increased upon Kv1.1−/−, could indicate that this increase may be localized to the hippocampus rather than the cortex (Fig. 5). The hippocampus is typically regarded as a “seizure gate” or controls seizure initiation (Barbarosie and Avoli 1997; Bragin et al. 1999). This suggests that seizure activity must be initiated in the hippocampus before it spreads to cortical regions. Further, Kv1.1 channels are densely clustered at the juxtaparanodal region close to the nodes of Ranvier and at axonal initial segments as these sites are responsible for action potential initiation (Robbins and Tempel 2012). Kv1.1 channels at these regions serve to limit excitatory activity. Additionally, lipid accumulation upon seizure induction and propagation has been observed along with an increase in phospholipase enzyme activity (Bazan et al. 2002). This may explain the upregulation of various glycerophospholipids, specifically phosphocholine and phosphoethanolamine in the hippocampus as it could reflect an elevated inflammatory response to seizure initiation and propagation. Subsequently, the pathways affected in the Kv1.1−/− were glycerophospholipid, sphingolipid, and glycosylphosphatidylinositol (GPI)-anchor biosynthesis (Fig. 4). By affecting these pathways, the subsequent impacts on membrane maintenance and signaling could aid in hyperexcitation.

In the brain, phospholipids maintain the neuronal integrity through regulating ion channel function and by supplying the brain’s energetic needs, and thus are critical to controlling neuronal excitation (Oliver et al. 2004). Approximately 20% of the brain’s energy requirements are generated through fatty acid oxidation, which takes place in the mitochondrial matrix (Ebert et al. 2003; Tracey et al. 2018). In other neurological conditions such as ALS, mitochondria become damaged, glucose is not a preferred fuel source, and lipid catabolic activity increases (Magrané et al. 2014, Dodge et al. 2013). Thus, the changes observed in the lipidome of the Kv1.1−/− model of epilepsy could be explained by changes in metabolic activity and/or compromised structural integrity in cellular membranes. It was demonstrated that the increase in adrenergic activity in seizures results in a decrease in lipogenic activity (Botion and Doretto 2003). Phospholipids account for a majority of lipid composition in cellular membranes. Changes in membrane structure could result in hyperexcitability through ion channels and pumps. In the hippocampus, PE was commonly upregulated, a lipid critical to membrane fluidity and metabolism. Increased PE was observed to increase fluidity of the membrane which could cause changes in vesicular transport (i.e. glutamate and GABA) (Thiam et al. 2013). Further, PE can be synthesized in

and localized to the mitochondria where it was shown to be critical for the cytochrome bc1 complex function which is responsible for ATP synthesis (Calzada et al. 2019). The changes observed in the lipidome may be consequential of required increase in ATP production to meet energetic demands of seizure activity (Wasterlain et al. 2010). Given the KD's effectiveness in seizure attenuation, it would be important to see the KD's further impacts on the epileptic hippocampal and cortical neurochemical makeup.

5 Conclusion

In conclusion, FT-ICR/MS was employed to examine changes in the lipidome associated with a Kv1.1 KO model of epilepsy. The presented study finds changes in overall lipid distribution between the hippocampus and cortex in this model. The general consequences of this change result in loss of membrane integrity and synaptic signaling changes. Specifically, our study suggests that increased levels of CL in the hippocampus may be indicative of seizure initiation and altered mitochondrial function upon Kv1.1 KO. The limitations of this study include limited sample sizes (n = 5 per condition) which does not allow for biomarker determination and limited ability for PLS-DA evaluation. Additionally, the lack of access to MS/MS fragmentation at time of data collection means that any IDs provided above are only tentative and *not* putative. Nonetheless, this study provides one of few descriptions of general changes in lipid metabolism associated with epilepsy and may open potential avenues for development of new therapies.

Supplementary Material

Refer to Web version on PubMed Central for supplementary material.

Acknowledgements

This work was supported by grants from the National Institute of Health (P20 RR017675, P20 GM104320, NS085389, NS072179 and NS111389) and from Citizens United for Research in Epilepsy Foundation.

References

Baek BS, Kwon HJ, Lee KH, Yoo MA, Kim KW, Ikeno Y, et al. (1999). Regional difference of ROS generation, lipid peroxidaton, and antioxidant enzyme activity in rat brain and their dietary modulation. Archives of Pharmacal Research, 22(4), 361–366. 10.1007/bf02979058. [PubMed: 10489874]

Barbarosie M, & Avoli M (1997). CA3-driven hippocampal-entorhinal loop controls rather than sustains in vitro limbic seizures. The Journal of Neuroscience, 17(23), 9308–9314. 10.1523/jneurosci.17-23-09308.1997. [PubMed: 9364076]

Bazan NG, Tu B, & Turco EBRD (2002). What synaptic lipid signaling tells us about seizure-induced damage and epileptogenesis. Progress in Brain Research, 135, 175–185. 10.1016/s0079-6123(02)35017-9. [PubMed: 12143339]

Botion LM, & Doretto MC (2003). Changes in peripheral energy metabolism during audiogenic seizures in rats. Physiology & Behavior, 78(4–5), 535–541. 10.1016/s0031-9384(03)00061-1. [PubMed: 12782206]

Bragin A, Engel J, Wilson CL, Fried I, & Mathern GW (1999). Hippocampal and entorhinal cortex high-frequency oscillations (100–500 Hz) in human epileptic brain and in kainic acid-treated rats with chronic seizures. Epilepsia, 40(2), 127–137. 10.1111/j.1528-1157.1999.tb02065.x. [PubMed: 9952257]

Calzada E, Avery E, Sam PN, Modak A, Wang C, Mccaffery JM, et al. (2019). Phosphatidylethanolamine made in the inner mitochondrial membrane is essential for yeast cytochrome bc1 complex function. Nature Communications. 10.1038/s41467-019-09425-1.

Chong J, Wishart DS, & Xia J (2019). Using MetaboAnalyst 4.0 for comprehensive and integrative metabolomics data analysis. Current Protocols in Bioinformatics. 10.1002/cpbi.86.

Dodge JC, Treleaven CM, Fidler JA, Tamsett TJ, Bao C, Searles M, et al. (2013). Metabolic signatures of amyotrophic lateral sclerosis reveal insights into disease pathogenesis. Proceedings of the National Academy of Sciences of the USA, 110, 10812–10817. 10.1073/pnas.1308421110. [PubMed: 23754387]

Ebert D, Haller RG, & Walton ME (2003). Energy contribution of octanoate to intact rat brain metabolism measured by 13C nuclear magnetic resonance spectroscopy. Journal of Neuroscience, 23, 5928–5935. [PubMed: 12843297]

Farooqui AA, Horrocks LA, & Farooqui T (2000). Glycerophospholipids in brain: their metabolism, incorporation into membranes, functions, and involvement in neurological disorders. Chemistry and Physics of Lipids, 106(1), 1–29. 10.1016/s0009-3084(00)00128-6. [PubMed: 10878232]

Fenoglio-Simeone KA, Wilke JC, Milligan HL, Allen CN, Rho JM, & Maganti RK (2009). Ketogenic diet treatment abolishes seizure periodicity and improves diurnal rhythmicity in epilepticKcna1-null mice. Epilepsia, 50(9), 2027–2034. 10.1111/j.1528-1167.2009.02163.x. [PubMed: 19490051]

Folch J, Lees M, & Stanley GHS (1957). A simple method for the isolation and purification of total lipides from animal tissues. Journal of Biological Chemistry, 226(1), 497–509. [PubMed: 13428781]

Guzman PD, Dantuono M, & Avoli M (2004). Initiation of electrographic seizures by neuronal networks in entorhinal and perirhinal cortices in vitro. Neuroscience, 123(4), 875–886. 10.1016/j.neuroscience.2003.11.013. [PubMed: 14751281]

Huttenlocher PR (1976). Ketonemia and seizures: Metabolic and anticonvulsant effects of two ketogenic diets in childhood epilepsy. Pediatric Research, 10(5), 536–540. 10.1203/00006450-197605000-00006. [PubMed: 934725]

Jernerén F, Söderquist M, & Karlsson O (2015). Post-sampling release of free fatty acids—Effects of heat stabilization and methods of euthanasia. Journal of Pharmacological and Toxicological Methods, 71, 13–20. 10.1016/j.vascn.2014.11.001. [PubMed: 25463283]

Ji J, Kline AE, Amoscato A, Samhan-Arias AK, Sparvero LJ, Tyurin VA, et al. (2012). Lipidomics identifies cardiolipin oxidation as a mitochondrial target for redox therapy of brain injury. Nature Neuroscience, 15(10), 1407–1413. 10.1038/nn.3195. [PubMed: 22922784]

Kalilani L, Sun X, Pelgrims B, Noack-Rink M, & Villanueva V (2018). The epidemiology of drug-resistant epilepsy: A systematic review and meta-analysis. Epilepsia, 59(12), 2179–2193. 10.1111/epi.14596. [PubMed: 30426482]

Kelly KM, & Chung SS (2011). Surgical treatment for refractory epilepsy: Review of patient evaluation and surgical options. Epilepsy Research and Treatment, 2011, 1–10. 10.1155/2011/303624.

Kim DY, Simeone KA, Simeone TA, Pandya JD, Wilke JC, Ahn Y, et al. (2015). Ketone bodies mediate antiseizure effects through mitochondrial permeability transition. Annals of Neurology, 78(1), 77–87. 10.1002/ana.24424. [PubMed: 25899847]

Kunduri G, Turner-Evans D, Konya Y, Izumi Y, Nagashima K, Lockett S, et al. (2018). Defective cortex glia plasma membrane structure underlies light-induced epilepsy in cpes mutants. Proceedings of the National Academy of Sciences. 10.1073/pnas.1808463115.

Lutas A, & Yellen G (2013). The ketogenic diet: Metabolic influences on brain excitability and epilepsy. Trends in Neurosciences, 36(1), 32–40. 10.1016/j.tins.2012.11.005. [PubMed: 23228828]

Magrané J, Cortez C, Gan WB, & Manfredi G (2014). Abnormal mitochondrial transport and morphology are common pathological denominators in SOD1 and TDP43 ALS mouse models. Human Molecular Genetics, 23, 1413–1424. 10.1093/hmg/ddt528. [PubMed: 24154542]

Mcdonald T, Puchowicz M, & Borges K (2018). Impairments in oxidative glucose metabolism in epilepsy and metabolic treatments thereof. Frontiers in Cellular Neuroscience. 10.3389/fncel.2018.00274.

Miranda AM, Bravo FV, Chan RB, Sousa N, Paolo GD, & Oliveira TG (2019). Differential lipid composition and regulation along the hippocampal longitudinal axis. Translational Psychiatry. 10.1038/s41398-019-0478-6.

Naudí A, Cabré R, Jové M, Ayala V, Gonzalo H, Portero-Otín M, et al. (2015). Lipidomics of human brain aging and Alzheimers disease pathology. International Review of Neurobiology Omic Studies of Neurodegenerative Disease: Part B. 10.1016/bs.irn.2015.05.008.

Nichols CG (2006). KATP channels as molecular sensors of cellular metabolism. Nature, 440(7083), 470–476. 10.1038/nature04711. [PubMed: 16554807]

Oliver D, Lien C, Soom M, Baukrowitz T, Jonas P, & Fakler B (2004). Functional conversion between A-type and delayed rectifier K channels by membrane lipids. Science, 304(5668), 265–270. 10.1126/science.1094113. [PubMed: 15031437]

Oliveros JC (2007). VENNY. An interactive tool for comparing lists with Venn Diagrams. Retrieved from http://bioinfogp.cnb.csic.es/tools/venny/index.html.

Paradies G, Paradies V, Benedictis VD, Ruggiero FM, & Petrosillo G (2014). Functional role of cardiolipin in mitochondrial bioenergetics. Biochimica Et Biophysica Acta (BBA) - Bioenergetics, 1837(4), 408–417. 10.1016/j.bbabio.2013.10.006. [PubMed: 24183692]

Pearson-Smith J, & Patel M (2017). Metabolic dysfunction and oxidative stress in epilepsy. International Journal of Molecular Sciences, 18(11), 2365. 10.3390/ijms18112365. [PubMed: 29117123]

Pluskal T, Castillo S, Villar-Briones A, & Oresic M (2010). MZmine 2: modular framework for processing, visualizing, and analyzing mass spectrometry-based molecular profile data. BMC Bioinform, 11, 395–395. 10.1186/1471-2105-11-395.

Robbins CA, & Tempel BL (2012). Kv1.1 and Kv1.2: similar channels, different seizure models. Epilepsia, 53, 134–141. 10.1111/j.1528-1167.2012.03484.x.

Roundtree HM, Simeone TA, Johnson C, Matthews SA, Samson KK, & Simeone KA (2016). Orexin receptor antagonism improves sleep and reduces seizures in Kcna1-null mice. Sleep, 39(2), 357–368. 10.5665/sleep.5444. [PubMed: 26446112]

Shirai Y, & Saito N (2014). Diacylglycerol kinase as a possible therapeutic target for neuronal diseases. Journal of Biomedical Science, 21(1), 28. 10.1186/1423-0127-21-28. [PubMed: 24708409]

Simeone KA, Matthews SA, Samson KK, & Simeone TA (2014a). Targeting deficiencies in mitochondrial respiratory complex I and functional uncoupling exerts anti-seizure effects in a genetic model of temporal lobe epilepsy and in a model of acute temporal lobe seizures. Experimental Neurology, 251, 84–90. 10.1016/j.expneurol.2013.11.005. [PubMed: 24270080]

Simeone TA, Samson KK, Matthews SA, & Simeone KA (2014b). In vivo ketogenic diet treatment attenuates pathologic sharp waves and high frequency oscillations in in vitro hippocampal slices from epileptic Kv1.1α knockout mice. Epilepsia. 10.1111/epi.12603.

Sooderberg M, Edlund C, Alafuzoff I, Kristensson K, & Dallner G (1992). Lipid composition in different regions of the brain in Alzheimers disease/senile dementia of Alzheimers type. Journal of Neurochemistry, 59(5), 1646–1653. 10.1111/j.1471-4159.1992.tb10994.x. [PubMed: 1402910]

Stas JI, Bocksteins E, Jensen CS, Schmitt N, & Snyders DJ (2016). The anticonvulsant retigabine suppresses neuronal KV2-mediated currents. Scientific Reports. 10.1038/srep35080.

Sud M, Fahy E, Cotter D, Brown A, Dennis EA, Glass CK, et al. (2007). LMSD: LIPID MAPS structure database. Nucleic Acids Research. 10.1093/nar/gkl838.

Thiam AR, Farese RV Jr., & Walther TC (2013). The biophysics and cell biology of lipid droplets. Nature Reviews Molecular Cell Biology, 14, 775–786. 10.1038/nrm3699. [PubMed: 24220094]

Tracey TJ, Steyn FJ, Wolvetang EJ, & Ngo ST (2018). Neuronal lipid metabolism: multiple pathways driving functional outcomes in health and disease. Frontiers in Molecular Neuroscience, 11(10), 1–25. [PubMed: 29403353]

Turker S, Severcan M, Ilbay G, & Severcan F (2014). Epileptic seizures induce structural and functional alterations on brain tissue membranes. Biochimica Et Biophysica Acta (BBA)—Biomembranes, 1838(12), 3088–3096. 10.1016/j.bbamem.2014.08.025. [PubMed: 25194682]

Vismer MS, Forcelli PA, Skopin MD, Gale K, & Koubeissi MZ (2015). The piriform, perirhinal, and entorhinal cortex in seizure generation. Frontiers in Neural Circuits. 10.3389/fncir.2015.00027.

Wasterlain CG, Thompson KW, Suchomelova L, & Niquet J (2010). Brain energy metabolism during experimental neonatal seizures. Neurochemical Research, 35(12), 2193–2198. 10.1007/s11064-010-0339-4. [PubMed: 21136154]

Weljie AM, Meerlo P, Goel N, Sengupta A, Kayser MS, Abel T, et al. (2015). Oxalic acid and diacylglycerol 36:3 are cross-species markers of sleep debt. Proceedings of the National Academy of Sciences, 112(8), 2569–2574. 10.1073/pnas.1417432112.

Wenk MR (2005). The emerging field of lipidomics. Nature Reviews Drug Discovery, 4(7), 594–610. 10.1038/nrd1776. [PubMed: 16052242]

Wenzel HJ, Vacher H, Clark E, Trimmer JS, Lee AL, Sapolsky RM, et al. (2007). Structural consequences of Kcna1 gene deletion and transfer in the mouse hippocampus. Epilepsia, 48(11), 2023–2046. 10.1111/j.1528-1167.2007.01189.x. [PubMed: 17651419]

Wishart DS, Feunang YD, Marcu A, Guo AC, Liang K, Vázquez-Fresno R, et al. (2017). HMDB 4.0: the human metabolome database for 2018. Nucleic Acids Research. 10.1093/nar/gkx108.

Zhang M, Mileykovskaya E, & Dowhan W (2005). Cardiolipin is essential for organization of complexes III and IV into a supercomplex in intact yeast mitochondria. Journal of Biological Chemistry, 280(33), 29403–29408. 10.1074/jbc.m504955200. [PubMed: 15972817]

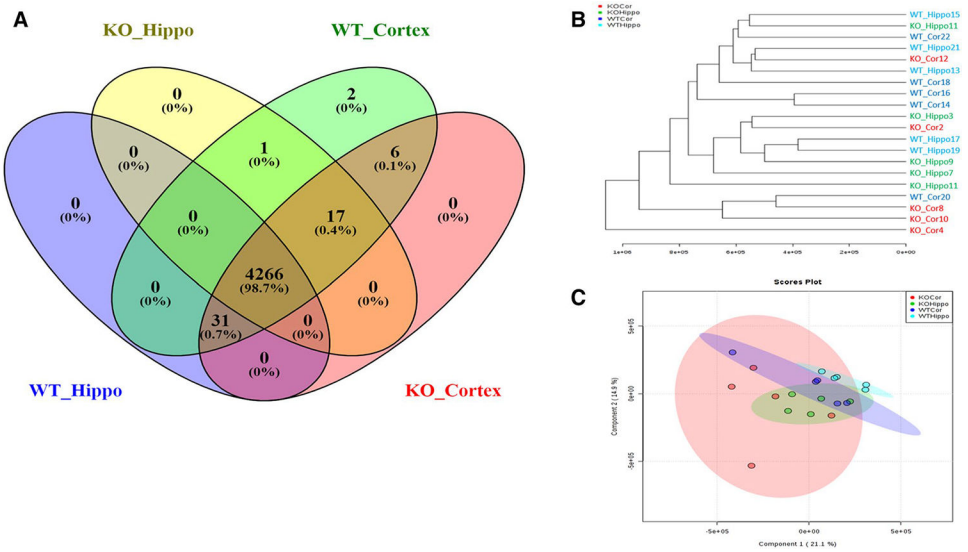

Fig. 1.

a Venn Diagram showing the uniqueness and overlap of all features. **b** Hierarchical clustering based on all features from each tissue. **c** PLS-DA score plots comparing the lipidomic profiles between hippocampal and cortical tissue in addition to wild-type vs. KV1.1−/−

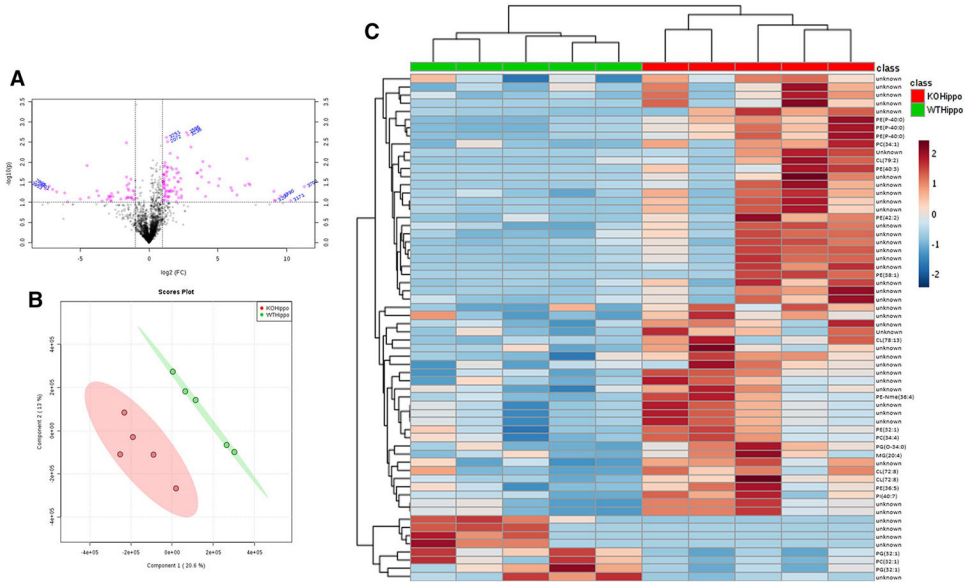

Fig. 2.

a Volcano plot of all features in the hippocampus. Compounds with a log2 fold change of > 2 (KO/WT) and a p value < 0.05 have been highlighted in pink. **b** PLS-DA scores plots comparing lipidomic profiles between Kv1.1−/− and WT mice in the hippocampus. **c** Heatmap detailing significant features in the hippocampus and the overall trend of upregulation in response to Kv1.1 knockout. Correlation of these features can also be seen by hierarchical clustering

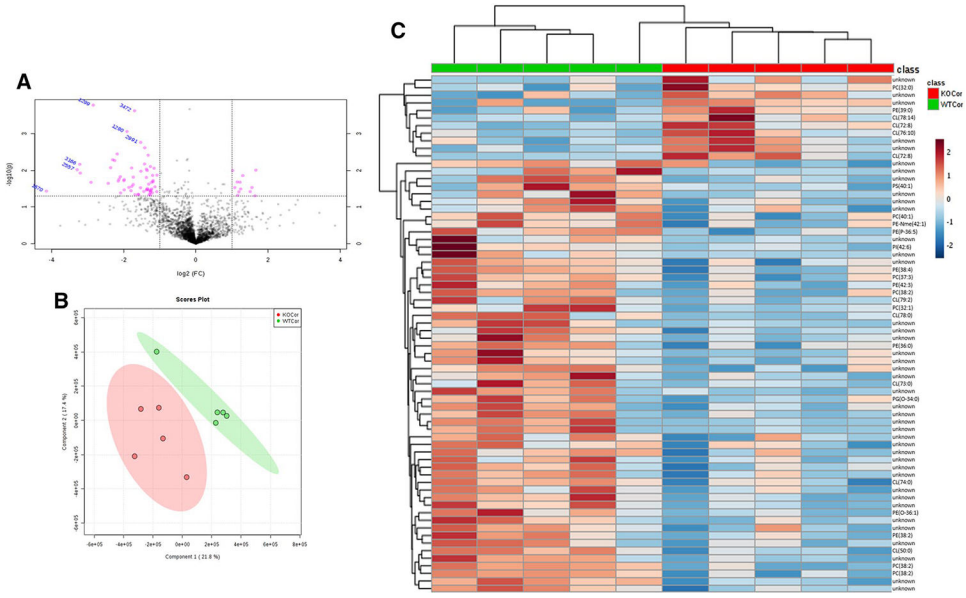

Fig. 3.

a Volcano plot of all features in the cortex. Compounds with a log2 fold change (KO/WT) of > 2 and a p value < 0.05 have been highlighted in pink. **b** PLS-DA scores plot comparing lipid changes in Kv1.1−/− and WT cortex tissue in mice. **c** Heatmap detailing significant features found in the cortex and overall trend of downregulation in response to Kv1.1 knockout. Correlation of these features are also shown by hierarchical clustering

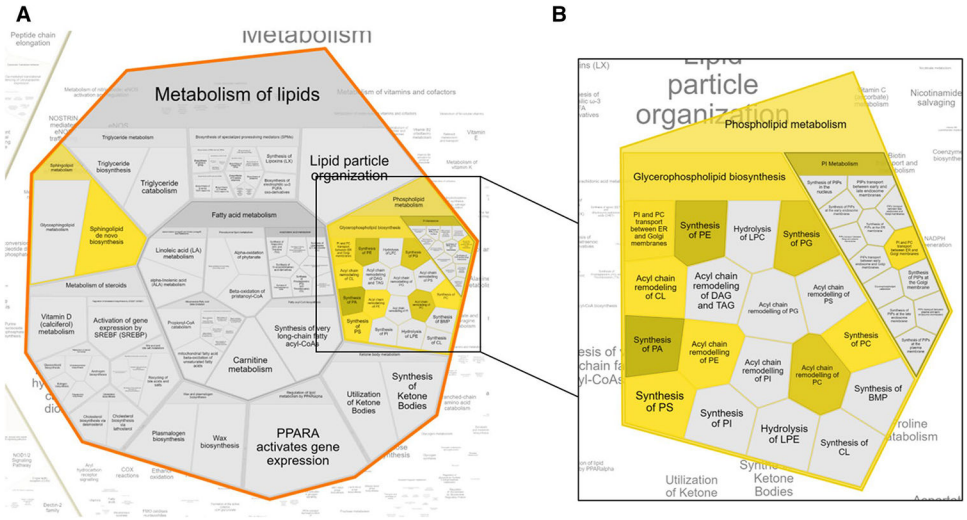

Fig. 4.

a Affected pathways generated from KEGG ID input show that overall metabolism of lipids is impacted. **b** Phospholipid metabolic pathways comprise a majority of lipid metabolism pathways affected, namely synthesis and remodeling pathways. All pathways highlighted are significant (adjusted $p < 0.05$)

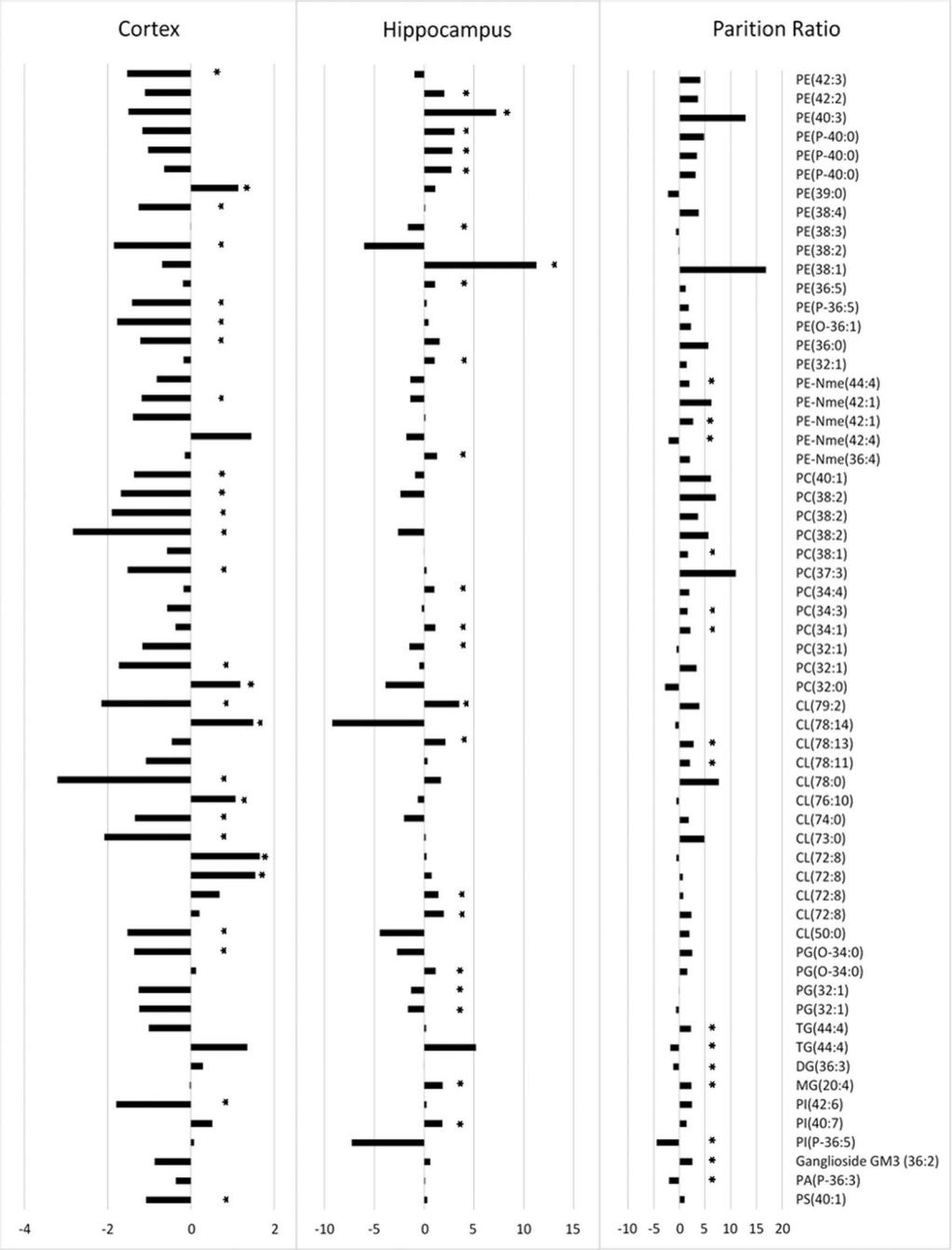

Fig. 5.

Comprehensive look of all tentatively identified significant lipid species found in each analysis described in this study and their respective fold changes (i.e. cortex, tissue, and partition ratio). "*" indicates that the species in question was significantly ($p < 0.05$) changed within the specified group only. All Fold Changes expressed as Log2 fold change

Table 1

Metabolites with significant ($p < 0.05$) change in partition ratio. Ratios expressed as average of all mice within genotype (i.e. KOHippo/KOCortex) (n = 5)

Feature#	M/z	RT	p value	FC	Log2(FC)	KOHippo/ KOCortex	WTHippo/ WTCortex	ID
2245	1541.0223	28.39342	0.000907	6.8923	2.785	1.48200753	0.215023588	CL(78:13)
2339	1545.0439	30.19693	0.006922	4.262	2.0915	1.463586611	0.343399848	CL(78:11)
1540	619.52859	21.45607	0.009393	0.437	− 1.1943	0.830521446	1.900523832	DG(36:3)
3076	914.54252	24.67435	0.01232	3.036	1.6022	1.691953198	0.557299834	
3266	1224.8029	28.47826	0.015475	2.9849	1.5777	2.661825002	0.891769288	
1161	1224.8033	27.96628	0.015729	2.5682	1.3608	2.39593153	0.932918216	
3750	760.58833	23.15106	0.017241	4.4833	2.1646	2.374186746	0.52956004	PC(34:1)
3717	760.63915	13.83236	0.019338	4.7603	2.2511	2.016014007	0.423501454	TG(44:4)
3362	683.5033	20.55179	0.020438	0.24804	− 2.0114	0.480660008	1.937868963	PA(P-36:3)
2924	1525.1976	15.98834	0.020848	2.4234	1.277	2.210609887	0.912186112	
2082	379.28289	24.94067	0.021525	5.0457	2.3351	1.036299124	0.205382444	MG(20:4)
2660	844.67999	36.38692	0.024484	6.4056	2.6793	5.12294113	0.799755633	PE-Nme(42:1)
2579	738.03114	17.5781	0.025059	3.1307	1.6465	3.367349222	1.075576499	
1108	1208.3911	24.68311	0.026134	2.6287	1.3943	2.288052422	0.870420822	
2972	1196.7696	34.11828	0.026748	5.7922	2.5341	2.749256348	0.474646828	Ganglioside GM3 (36:2)
3661	841.53216	30.91421	0.027573	0.047042	− 4.4099	0.00990206	0.126812919	PI(P-36:5)
3472	914.54248	24.59988	0.027738	3.6168	1.8547	1.832314343	0.506609079	
1470	1524.1937	15.97183	0.027769	3.1886	1.6729	3.744400781	1.174307862	
3510	1233.8481	31.37504	0.028188	0.10502	− 3.2513	0.022294484	0.127725196	
2665	760.64102	14.68543	0.029931	0.29305	− 1.7708	1.45868118	4.977511093	TG(44:4)
3517	1497.0355	35.23429	0.031846	2.9383	1.555	1.353905614	0.460785799	
4030	838.63259	14.46687	0.039145	0.23455	− 2.092	0.984924332	4.19924118	PE-Nme(42:4)
1682	756.55241	15.49642	0.039495	3.0165	1.5929	1.894507631	0.62804463	PC(34:3)
1164	1520.1638	33.82245	0.040437	2.2832	1.1911	1.017646038	0.445704607	
4280	1148.7733	34.60997	0.040507	4.3776	2.1301	4.343095949	0.992120507	
3708	866.66418	17.30173	0.041693	3.9187	1.9704	2.445672862	0.6240973	PE-Nme(44:4)
4277	936.73614	25.33598	0.043101	0.44316	− 1.1741	1.070164227	2.414839826	
1671	816.63931	16.1634	0.046744	3.1983	1.6773	2.329997034	0.728515739	PC(38:1)
2670	869.65258	21.9099	0.049855	2.2549	1.173	2.156816436	0.956515904	

*Provided annotation represent simple m/z based fit and can be affected by in source fragmentation. Therefore, it is important to note that all identifications are tentative, and their validation would require additional characterization involving purified standards and extensive MS^n analysis